Ocean Engineering 279 (2023) 114602

Contents lists available at ScienceDirect

Ocean Engineering

journal homepage: www.elsevier.com/locate/oceaneng

An advanced prediction method of ship resistance with heterogeneous hull roughness

Soonseok Song [a], Daejeong Kim [b,*], Yigit Kemal Demirel [c], Jungkyu Yang [a,d]

[a] Department of Naval Architecture & Ocean Engineering, Inha University, South Korea
[b] Department of Naval Architecture, Ocean & Marine Engineering, University of Strathclyde, UK
[c] C/Raval de Gracia, Cambrils, Tarragona, 43850, Spain
[d] Defense Acquisition Program Administration, South Korea

ARTICLE INFO

Handling Editor: Prof. A.I. Incecik

Keywords:
Ship resistance
Roughness effect
Biofouling
Heterogeneous hull roughness
Similarity law scaling

ABSTRACT

Despite the ongoing efforts for predicting the effect of hull roughness on ship resistance, the majority of the studies have been treating the hull surfaces as uniformly (i.e., homogeneously) rough. This can be a limiting factor since the real ships' hulls are not uniform due to various reasons such as the heterogeneous accumulation of biofouling. The current study aims to propose a new prediction method for added resistance due to heterogeneous hull roughness. This newly proposed method incorporates the similarity law scaling and the Roughness Impact Factor to consider the relative impacts of hull roughness in different regions. Two separate case studies involving recent Experimental Fluid Dynamics (EFD) and Computational Fluid Dynamics (CFD) results were used to assess the newly proposed method, which showed better prediction performance compared to the conventional method.

1. Introduction

While developing new technologies to decarbonize maritime transport is essential to achieve IMO's Greenhouse Gas Strategy towards 2050, it is equally important to optimize the energy efficiency of existing ships. The main factor deteriorating ships' energy efficiency in service is the undesirable accumulation of biological matter on the ship hull surfaces, which is often called "biofouling". Within this context, predicting the penalty in ships' energy efficiency due to biofouling is of critical importance. As such, there have been studies modelling the effect of biofouling on ship performances using experimental, (Demirel et al., 2017b; Hutchins et al., 2016; Schultz, 2000, 2004; Schultz et al., 2003; Schultz et al., 2000; Schultz et al., 2015; Song et al., 2021a, 2021c; Turan et al., 2016; Uzun et al., 2020), numerical (Demirel et al., 2014, 2017a; Farkas et al., 2018, 2020b, 2019; 2020a; 2021; Owen et al., 2018; Song et al., 2019, 2020c, 2020d, 2020e, 2021b, 2020a; 2020b; Suastika et al., 2021) and theoretical methods (Demirel et al., 2017b; Schultz, 2004, 2007; Schultz et al., 2011; Song et al., 2021a; Uzun et al., 2019a, 2019b).

Despite these active efforts, there is still a limiting factor. Within these studies, the hull surfaces were assumed to be uniform for simplicity. However, this assumption may degrade the prediction accuracy, because the hull surfaces of real ships are not homogeneous due to various factors such as the heterogeneous nature of the biofouling accumulation. Furthermore, ship owners occasionally choose partial hull cleanings, which contributes to the hulls' heterogeneity. Song et al. (2021c) experimentally demonstrated how the impacts of hull roughness can differ depending on the locations of hull roughness. Their results suggest that the hull roughness of the front part of the ship results in greater added resistance than the hull roughness in other regions. In a later work, they showed that the influence of heterogeneous hull roughness can be modelled in Computational Fluid Dynamics (CFD) simulations and reasoned that the different roughness Reynolds number distribution on different hull regions are the main cause of the different impacts (Song et al., 2021b). Recently, Ravenna et al. (2022) proposed a new measure called "Roughness Impact Factor", *RIF* to quantify the impacts of heterogeneous hull roughness varying with the rough surfaces' position. Moreover, they performed CFD simulations to determine the *RIF* values of different hull regions of a model-scale containership.

While these studies on heterogeneous hull roughness offer useful insights, there is currently no practical method to predict the added resistance due to heterogeneous hull roughness. The aim of the current study is, therefore, to propose a new method to accurately predict the added resistance owing to heterogeneous hull roughness. The newly

* Corresponding author.
E-mail address: daejeong.kim@strath.ac.uk (D. Kim).

https://doi.org/10.1016/j.oceaneng.2023.114602
Received 3 January 2023; Received in revised form 4 April 2023; Accepted 14 April 2023

proposed prediction method incorporates the similarity law scaling of Granville (1958) and the Roughness Impact Factor, *RIF*, values on different hull regions to effectively weigh up the relative impacts of hull roughness in different regions. Two case studies were performed to assess the newly proposed method: One involving the recent experiment of Song et al. (2021c) and one involving the CFD simulations of Ravenna et al. (2022). The case studies revealed that the newly proposed method outperformed the conventional method, indicating that the use of proposed method has a potential to improve the ship resistance predictions with heterogeneous hulls.

2. Methodology

2.1. Roughness impact factor

Ravenna et al. (2022) presented a new measure called "Roughness Impact Factor, *RIF* to assess the relative impacts of heterogeneous hull roughness. In the determination process of the *RIF*, a hull surface consisting of n surface regions ($i = 1,2,3,\dots,n$) is considered. When the i th surface is rough while the other regions remain smooth, the roughness impact factor of the i th surface, RIF_i, is determined as follows:

$$RIF_i = \frac{\Delta C_{T,i} / WSA_i}{\Delta C_{T,Full\ Rough} / WSA_{Total}} \tag{1}$$

in which $\Delta C_{T,i}$ is the added resistance due to the hull roughness of the i th surface. $\Delta C_{T,Full\ Rough}$ is the added resistance when the entire hull is covered with the given roughness. WSA_i and WSA_{Total} are the wetted surface area of the i th surface region and the entire submerged area of the hull, respectively. In this quantification method, *RIF* value of unity indicates that the corresponding surface has an average impact. A value of $RIF > 1$ indicates that the corresponding region has a greater impact than the average of all regions. Similarly, a value of $RIF < 1$ suggests that the region has a lower impact than the average.

2.2. New prediction method for added resistance due to heterogeneous hull roughness

Song et al. (2021c) suggested a simple method to predict the added resistance due to heterogeneous hull roughness based on the similarity law scaling of Granville (1958). Using this method, the added resistance due to heterogeneous hull roughness, $\Delta C_{F,hetero}$, can be calculated as follows:

$$\Delta C_{F,hetero} = \sum_{i=1}^{n} \frac{WSA_i}{WSA_{ship}} \Delta C_{F,i} \tag{2}$$

$\Delta C_{F,i}$ is the added frictional resistance with the hull roughness in the i^{th} region obtained from Granville's method ($i = 1, 2, \dots, n$), under the assumption of the homogeneous distribution of the given roughness over the whole hull. Details of Granville's similarity law scaling can be found in our previous studies (Demirel et al., 2017b; Song et al., 2021a).

The frictional resistance of the ship $C_{F,r}$ with heterogeneous hull roughness can be determined as

$$C_{F,r} = C_{F,s} + \Delta C_F \tag{3}$$

in which, $C_{F,s}$ is the frictional resistance coefficient of a smooth ship that can be obtained by using the Kàrmàn-Schoenherr friction line (Schoenherr, 1932), as

$$\frac{0.242}{\sqrt{C_F}} = \log\left(Re_L C_F\right) \tag{4}$$

where, Re_L is the Reynolds number based on the length of the ship. As one may have noticed, this method only considers the effect of the different wetted surface area ratios of the individual roughness patches, rather than considering the effects of different positions of the roughness regions.

Table 1
Principal particulars of the Wigley hull model used for the experiment of Song et al. (2021c).

Length	L (m)	3.00
Beam at waterline	B (m)	0.30
Draft	T (m)	0.1875
Beam/draft ratio	B/T	1.6
Total wetted surface area	WSA (m^2)	1.3383
Wetted surface area of first quarter	WSA_{Q1} (m^2)	0.3066
Wetted surface area of first half	WSA_{H1} (m^2)	0.6691
Displacement	∇ (m^3)	0.0750
Block coefficient	C_B	0.4444
Towing speed	V (m/s)	1.08–2.71
Froude number	Fn	0.2–0.5
Reynolds number	Re_L	2.6–6.6 × 10^6
Water temperature	T_w (°C)	12

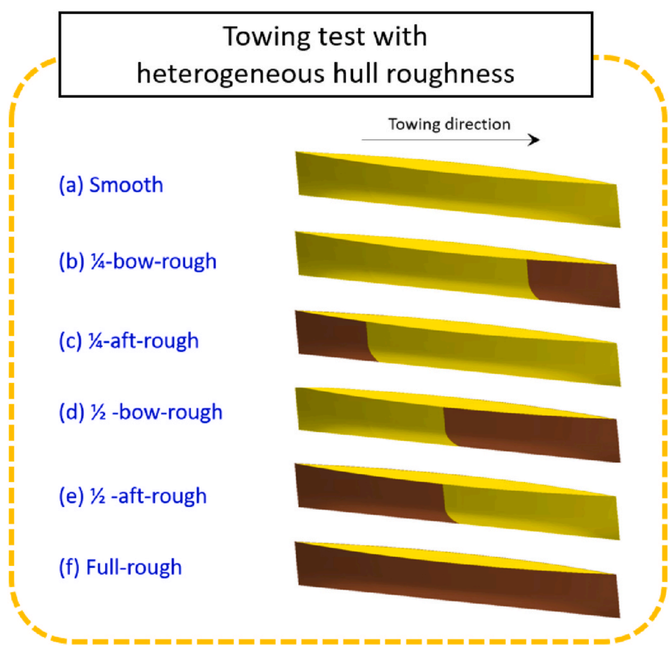

Fig. 1. Heterogeneous hull conditions used by the experiments of Song et al. (Song et al., 2021c).

Therefore, the current study proposes a novel method that improves the method of Song et al. (2021c) by including the roughness impact factor, RIF_i, in Equation (2). In other words, in this newly proposed method, the added resistance due to the heterogeneous hull roughness, $\Delta C_{F,hetero}$, can be predicted as follows:

$$\Delta C_{F,hetero} = \sum_{i=1}^{n} \frac{WSA_i}{WSA_{ship}} RIF_i \Delta C_{F,i} \tag{5}$$

Since the roughness impact factor, RIF_i, and the proportion of the wetted surface area of each patch are considered together, this new prediction approach can take into account the effects of the individual roughness patches' position and wetted surface area at the same time. Finally, the total resistance coefficient with the heterogeneous hull (i.e. $C_{T,hetero}$) can be determined as

$$\Delta C_{T,hetero} = (1+k)\Delta C_{F,hetero} \tag{6}$$

$$C_{T,hetero} = C_{T,s} + \Delta C_{T,hetero} \tag{7}$$

in which, $C_{T,s}$ is the total resistance coefficient of the ship with a clean hull. It is of note that, as per the conclusion of Song et al. (2021a), the

Table 2
FRI values calculated from the experimental data of Song et al. (2021c)

Re_L	Added resistance, ΔC_T			Roughness Impact Factor, *RIF*	
	Full-rough	¼-bow-rough	¼-aft-rough	Quartile 1*	Quartile 4*
2.64E+06	1.863E-03	7.161E-04	3.678E-04	1.678	0.8618
3.30E+06	2.018E-03	8.057E-04	2.983E-04	1.742	0.6452
3.95E+06	2.171E-03	8.781E-04	3.170E-04	1.765	0.6373
4.61E+06	2.428E-03	9.717E-04	3.824E-04	1.747	0.6873
5.27E+06	2.503E-03	8.811E-04	4.239E-04	1.537	0.7392
5.93E+06	2.861E-03	9.971E-04	5.080E-04	1.521	0.7750
6.59E+06	2.986E-03	9.739E-04	5.771E-04	1.424	0.8437

form factor, $1+k$, was used in this study to incorporate the roughness effect on the form resistance.

3. Results

3.1. Case study 1

In Case study 1, the proposed method was applied to the heterogeneous hull conditions of the Wigley hull used in the experiment of Song et al. (2021c). Song et al. (2021c) conducted a series of towing tests were conducted using a ship model of the Wigley hull with various hull roughness conditions, including homogeneous conditions (i.e. smooth and full-rough conditions) and heterogeneous conditions (i.e. ¼-bow-rough, ¼-aft-rough, ½-bow-rough and ½-aft-rough conditions). Table 1 and Fig. 1 show the principal particulars of the Wigley hull model and heterogeneous hull conditions used by Song et al. (2021c). For the rough surfaces, they coated the hull with 60/80 grit aluminium oxide abrasive powder (Rt_{50} = 353 μm).

It should be noted that Song et al. (2021c) did not calculate the *RIF* values in their study, as the concept of *RIF* introduced after this study. Therefore, *RIF* values of the Wigley hull were calculated in the current study using the equation (1), and reproducing the experimental data of Song et al. (2021c). Table 2 and Fig. 2 show the *RIF* values for the first and last quartiles (i.e. Quartiles 1 and 4) with different speeds (i.e. Re_L). As shown in Fig. 2 the *RIF* values of the Quartiles 1 and 4 alter with the Reynolds number. It is worth mentioning that these *RIF* values indicate that the Quartile 1 experiences a maximum of 75% greater skin friction increase, while the Quartile 4 experiences up to a 35% smaller friction increase compared to the average. The *RIF* values of Quartile 1 show a decreasing trend as the Reynolds number increases, while that of Quartile 4 shows an increasing trend. These trends can be related to the transitional behaviors of the flow along the hull (e.g. laminar-turbulent transition and the smooth-rough transition), but further research is needed to confirm these characteristics.

Using the obtained *RIF* values and Equation (5) the added frictional resistance, ΔC_F, of the heterogeneous hull conditions were predicted. Fig. 3 shows the ΔC_F values of the ¼-bow-rough and ¼-aft-rough conditions, while the frictional resistance of these conditions ($C_{F,hetero} = C_{F,s} + \Delta C_F$) are shown in Fig. 4. In these figures, the "¼-rough" indicates the results obtained using the practical method of Song et al. (2021c), which does not consider the different positions of the roughness regions (i.e. Equation (2)). For this reason, the results for the ¼-rough conditions are found in between the results of ¼-bow-rough and ¼-aft-rough conditions. It is of note that the similarity law scaling was conducted based on the Nikuradse-type roughness function model of Cebeci and Bradshaw (1977) with the reference roughness height of $k = 1.73Rt_{50}$, as similarly done by Song et al. (2021a; 2021c). Evidently, the predicted ΔC_F and C_F values for the ¼-bow-rough condition are greater than the values for the ¼-aft-rough condition as a result of using the *RIF* values to incorporate the relative effects of roughness locations.

Using the obtained ΔC_F values, the total resistance of the Wigley hull with different hull conditions was predicted using Equation (6) with the form factor value of $1+k = 1.12$ as utilised by Song et al. (2021c). Fig. 5 shows the total resistance coefficients of the Wigley hull for the ¼-bow-rough and ¼-aft-rough conditions. It is worth noting that the predicted results indicate a good agreement with the experimental data, which suggests that incorporating the relative effects of hull roughness in different positions through the use of *RIF* has an impact on the accuracy of the predictions.

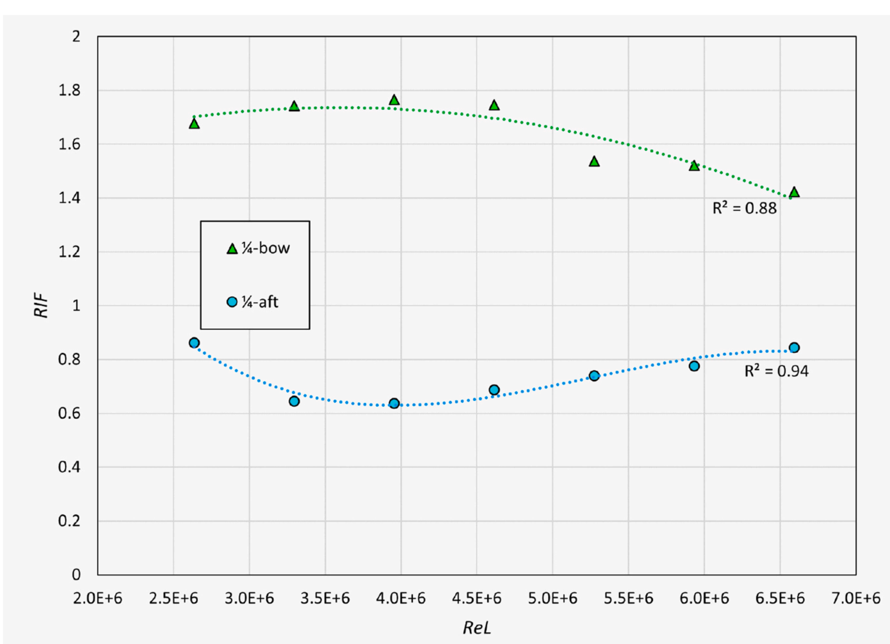

Fig. 2. Roughness Impact Factor, *RIF*, on the Quartiles 1 and 4 of the Wigley hull.

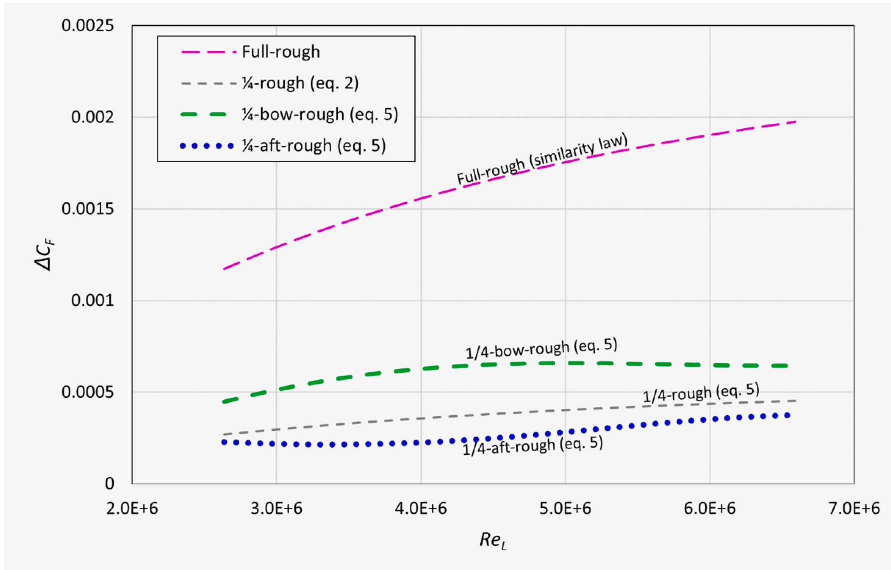

Fig. 3. Added frictional resistance coefficient for the heterogeneous hull conditions.

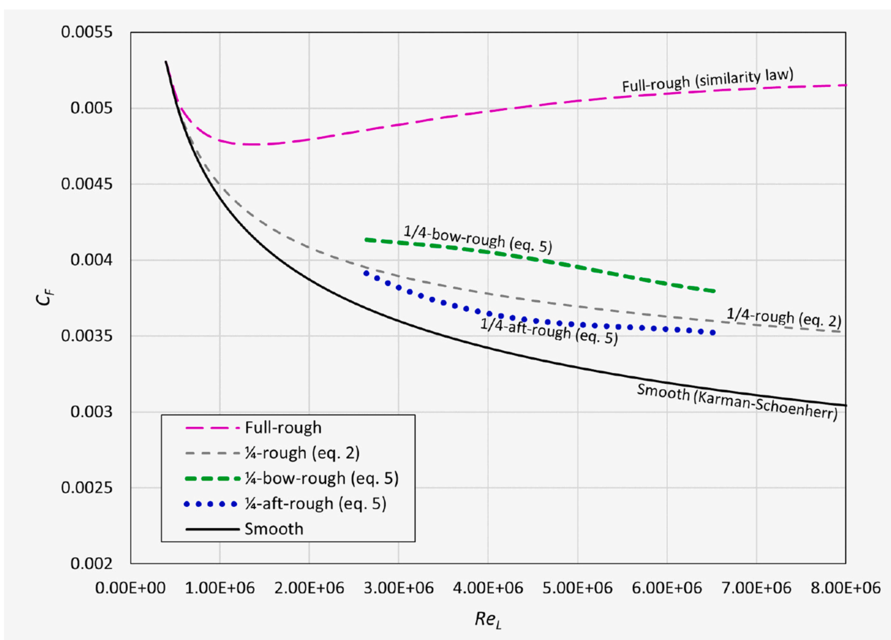

Fig. 4. Frictional resistance coefficient predicted from different methods.

3.2. Case study 2

In Case study 2, the proposed method was applied to the heterogeneous hull conditions of the KRISO Containership (KCS) model used in the CFD study of Ravenna et al. (2022). Table 3 shows the principal particulars of the KCS model used for the CFD simulations of Ravenna et al. (2022), while Fig. 6 shows the applied heterogeneous hull conditions, respectively. From the CFD simulations, Ravenna et al. (2022) calculated the total resistance under the different hull conditions and determined the Roughness Impact Factor, *RIF*, values on the different hull regions. Table 4 shows the percentages of the wetted surface area of the rough surfaces, $\%WSA_{Rough}$, for the different hull conditions and the corresponding *RIF* values obtained based on the CFD simulation results.

With the given data (i.e. $\%WSA_{Rough}$ and *RIF*), the added frictional resistance, ΔC_F, for the different hull conditions were predicted using two different methods: the practical method of Song et al. (2021c) that does not consider *RIF* (i.e. Equation (2)) and the newly proposed method using *RIF* (i.e. Equation (5)). The added total resistance coefficients were then determined utilizing equation (6) with the form factor value of $1 + k = 1.20$ (Van et al., 2011).

Table 5 and Fig. 7 show the added total resistance coefficients, ΔC_T, for the heterogeneous hull conditions predicted from the two different methods, while Fig. 8 shows the total resistance coefficients of the ship ($C_{T,hetero} = C_{T,smooth} + \Delta C_T$). The results show that the newly proposed method (i.e. Equation (5)) outperforms the practical method (i.e. Equation (2)). Particularly, the practical method gives large discrepancies for the roughness conditions with low $\%WSA_{Rough}$, while the newly proposed method consistently displays small discrepancies. For example, the errors of the ΔC_T prediction based on Equation (2) for the "*Bulbous bow*" and "*Stern*" scenarios are −55.34% and 127.83%,

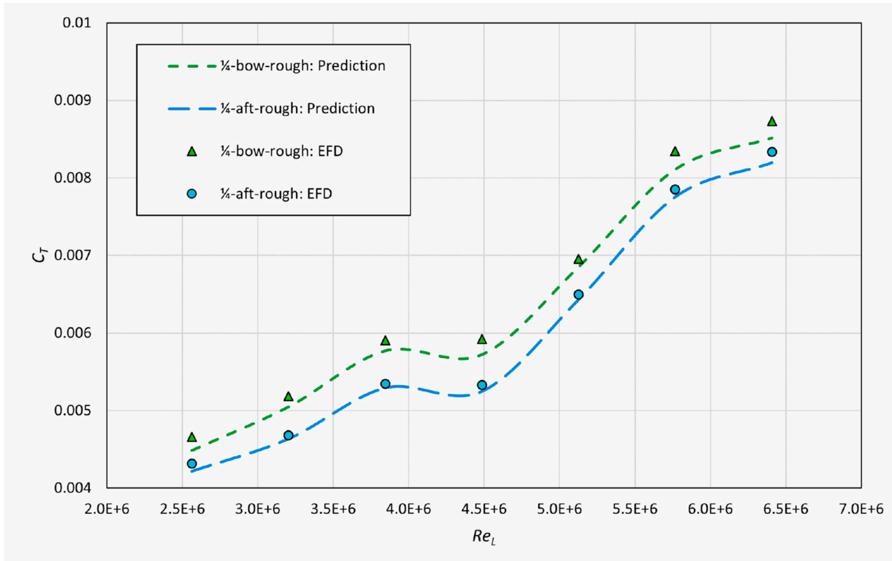

Fig. 5. Total resistance coefficients predicted from different methods and the experimental results.

respectively, and these errors are reduced to 0.54% and 0.25% by considering the *RIF* through Equation (5). It is noteworthy that these two methods yield identical results for the "*Full rough*" condition, where *RIF* is unity and thus Equation (5) becomes Equation (2) in this scenario.

Table 3
Principal particulars of the KCS model used in the study of Ravenna et al. (2022).

Parameters		Full-scale	Model-scale
Scale factor	λ	1	75
Length between the perpendiculars	L_{PP} (m)	230	3.0667
Length of waterline	L_{WL} (m)	232.5	3.1
Beam at waterline	B_{WL} (m)	32.2	0.4293
Depth	D (m)	19.0	0.2533
Design draft	T (m)	10.8	0.144
Wetted surface area w/o rudder	S (m^2)	9424	1.6753
Displacement	∇ (m^3)	52030	693.733
Block coefficient	C_B	0.6505	0.6505
Design speed	V (knot, m/s)	24	1.426
Froude number	F_n	0.26	0.26
Centre of gravity	KG (m)	7.28	0.0971
Metacentric height	GM (m)	0.6	0.008

Table 4
RIF values of different roughness regions used by Ravenna et al. (2022).

Roughness conditions	%Wetted surface area of the rough surface, $\%WSA_{Rough}$	Roughness Impact Factor, *RIF*
Bulbous bow	2.57%	2.26
Fore hull	17.68%	1.19
Midship	29.50%	1.18
Aft hull	19.13%	1.19
Stern	8.14%	0.44
Flat bottom	22.92%	0.85
Full rough	100%	1

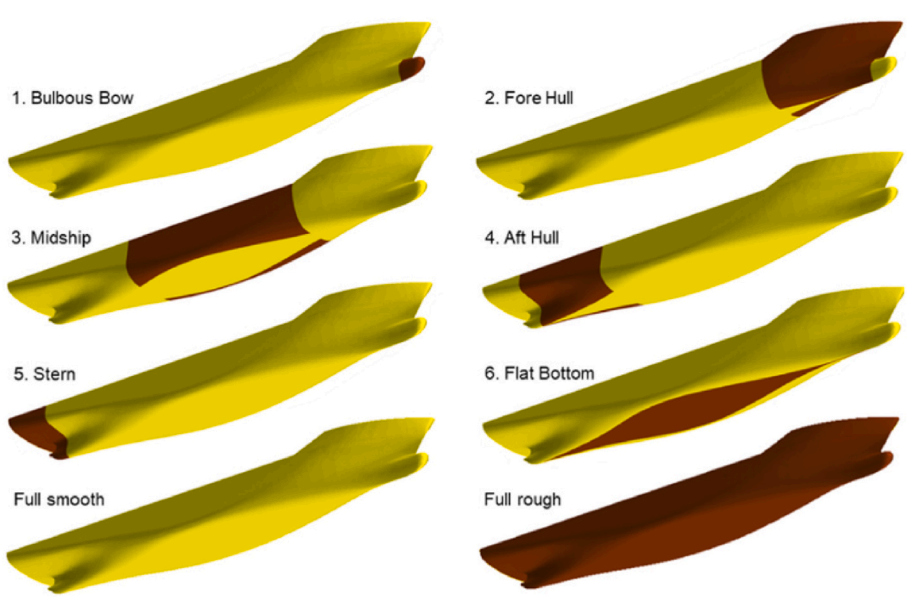

Fig. 6. Hull roughness conditions of the KCS model used by the study of Ravenna et al. (2022).

Table 5
Added total resistance coefficient predictions for heterogeneous hull conditions.

Roughness scenario	CFD (Ravenna et al., 2022)	Prediction without *RIF* (eq. (2))		Prediction with *RIF* (eq. (5))	
	ΔC_T	ΔC_T	Error	ΔC_T	Error
Bulbous bow	9.680E-05	4.323E-05	−55.34%	9.770E-05	0.93%
Fore hull	3.520E-04	2.974E-04	−15.51%	3.539E-04	0.54%
Midship	5.820E-04	4.962E-04	−14.74%	5.856E-04	0.61%
Aft hull	3.780E-04	3.218E-04	−14.87%	3.829E-04	1.31%
Stern	6.010E-05	1.369E-04	127.83%	6.025E-05	0.25%
Flat bottom	3.240E-04	3.855E-04	19.00%	3.277E-04	1.15%
Full rough	1.670E-03	1.682E-03	0.73%	1.682E-03	0.73%

4. Concluding remarks

In this work, a novel method was proposed to predict the added resistance due to heterogeneous hull roughness. This method incorporates the similarity law scaling and the Roughness Impact Factor, *RIF*, to consider the relative impacts of hull roughness in different regions. The newly proposed method was assessed through two case studies involving the results of recent Experimental Fluid Dynamics (EFD) and Computational Fluid Dynamics (CFD) studies (i.e. studies by Song et al. (2021c) and Ravenna et al. (2022), respectively). The results showed that the newly proposed method outperforms the conventional method as a result of considering the relative effects of hull roughness with different positions. Especially, the new approach was effective when a small portion of the hull is rough. Overall, the newly proposed method can improve the accuracy of resistance prediction for ships operating with unevenly fouled hulls, as well as predict the impacts of partial hull cleanings.

This study provides a novel approach for practical predictions of ship resistance with heterogeneous hull conditions. However, the prediction can only be made when the Roughness Reynolds Number, *RIF*, values are available. Furthermore, the *RIF* values can vary with different hull shapes and speeds. Therefore, future work shall be conducted to investigate the *RIF* values for different hull types to find the universal formula for the Roughness Reynolds Number.

It is worth mentioning that the hull conditions examined in this study were not entirely heterogeneous, but rather were produced by systematically combining homogeneous roughness patches. This approach was necessary to validate the newly proposed method. However, some may argue that such hull conditions may not an accurate representation of the real-world ship hulls conditions. As such, a potential avenue for future research could be the application of the proposed approach to actual ships with fully heterogeneous hulls.

CRediT authorship contribution statement

Soonseok Song: Data curation, Investigation, Formal analysis, Validation, Writing – review & editing, Funding acquisition, Project administration. **Daejeong Kim:** Formal analysis, Writing – review & editing. **Yigit Kemal Demirel:** Conceptualization, Methodology, Supervision, Writing – review & editing, Project administration. **Jung-Kyu Yang:** Formal analysis, Writing – review & editing.

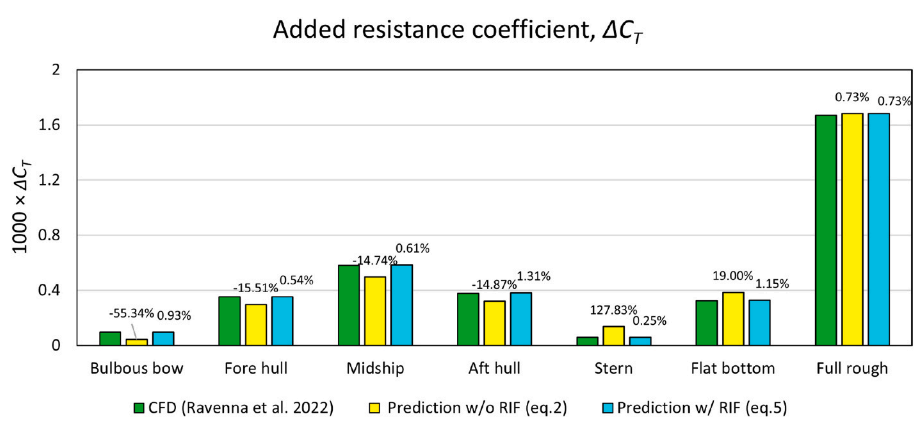

Fig. 7. Added total resistance coefficient predictions for heterogeneous hull conditions.

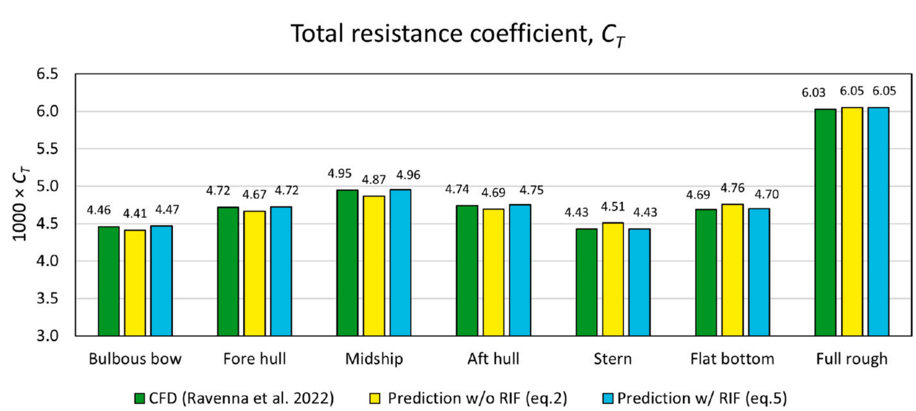

Fig. 8. Total resistance coefficient predictions for heterogeneous hull conditions.

Declaration of competing interest

The authors declare that they have no known competing financial interests or personal relationships that could have appeared to influence the work reported in this paper.

Data availability

The data that has been used is confidential.

Acknowledgements

This work was supported by the National Research Foundation of Korea(NRF) grant funded by the Korea government (MSIT) (No. RS-2022-00165770).

References

Cebeci, T., Bradshaw, P., 1977. Momentum Transfer in Boundary Layer, –1.

Demirel, Y.K., Khorasanchi, M., Turan, O., Incecik, A., Schultz, M.P., 2014. A CFD model for the frictional resistance prediction of antifouling coatings. Ocean Eng. 89, 21–31. https://doi.org/10.1016/j.oceaneng.2014.07.017.

Demirel, Y.K., Turan, O., Incecik, A., 2017a. Predicting the effect of biofouling on ship resistance using CFD. Appl. Ocean Res. 62, 100–118. https://doi.org/10.1016/j.apor.2016.12.003.

Demirel, Y.K., Uzun, D., Zhang, Y., Fang, H.-C., Day, A.H., Turan, O., 2017b. Effect of barnacle fouling on ship resistance and powering. Biofouling 33 (10), 819–834. https://doi.org/10.1080/08927014.2017.1373279.

Farkas, A., Degiuli, N., Martić, I., 2018. Towards the prediction of the effect of biofilm on the ship resistance using CFD. Ocean Eng. 167, 169–186. https://doi.org/10.1016/j.oceaneng.2018.08.055.

Farkas, A., Degiuli, N., Martić, I., 2019. Impact of biofilm on the resistance characteristics and nominal wake. Proc. IME M J. Eng. Marit. Environ. https://doi.org/10.1177/1475090219862897, 1475090219862897.

Farkas, A., Degiuli, N., Martić, I., 2020a. An investigation into the effect of hard fouling on the ship resistance using CFD. Appl. Ocean Res. 100, 102205 https://doi.org/10.1016/j.apor.2020.102205.

Farkas, A., Degiuli, N., Martić, I., 2021. The impact of biofouling on the propeller performance. Ocean Eng. 219, 108376 https://doi.org/10.1016/j.oceaneng.2020.108376.

Farkas, A., Song, S., Degiuli, N., Martić, I., Demirel, Y.K., 2020b. Impact of biofilm on the ship propulsion characteristics and the speed reduction. Ocean Eng. 199, 107033 https://doi.org/10.1016/j.oceaneng.2020.107033.

Granville, P.S., 1958. The frictional resistance and turbulent boundary layer of rough surfaces. J. Ship Res. 2 (3), 52–74.

Hutchins, N., Monty, J.P., Nugroho, B., Ganapathisubramani, B., Utama, I.K.A.P., 2016. Turbulent boundary layers developing over rough surfaces: from the laboratory to full-scale systems. In: Proceedings of the 20th Australasian Fluid Mechanics Conference, AFMC 2016.

Owen, D., Demirel, Y.K., Oguz, E., Tezdogan, T., Incecik, A., 2018. Investigating the effect of biofouling on propeller characteristics using CFD. Ocean Eng. https://doi.org/10.1016/j.oceaneng.2018.01.087.

Ravenna, R., Song, S., Shi, W., Sant, T., De Marco Muscat-Fenech, C., Tezdogan, T., Demirel, Y.K., 2022. CFD analysis of the effect of heterogeneous hull roughness on ship resistance. Ocean Eng. 258, 111733 https://doi.org/10.1016/j.oceaneng.2022.111733.

Schoenherr, K.E., 1932. Resistance of flat surfaces moving through a fluid. Trans SNAME 40, 279–313.

Schultz, M.P., 2000. Turbulent boundary layers on surfaces covered with filamentous algae. J. Fluid Eng. 122 (2), 357–363. https://doi.org/10.1115/1.483265.

Schultz, M.P., 2004. Frictional resistance of antifouling coating systems. J. Fluid Eng. 126 (6), 1039–1047. https://doi.org/10.1115/1.1845552.

Schultz, M.P., 2007. Effects of coating roughness and biofouling on ship resistance and powering. Biofouling 23 (5), 331–341. https://doi.org/10.1080/08927010701461974.

Schultz, M.P., Bendick, J.A., Holm, E.R., Hertel, W.M., 2011. Economic impact of biofouling on a naval surface ship. Biofouling 27 (1), 87–98. https://doi.org/10.1080/08927014.2010.542809.

Schultz, M.P., Myers, A., 2003. Comparison of three roughness function determination methods. Exp. Fluid 35 (4), 372–379. https://doi.org/10.1007/s00348-003-0686-x.

Schultz, M.P., Swain, G.W., 2000. The influence of biofilms on skin friction drag. Biofouling 15 (1–3), 129–139. https://doi.org/10.1080/08927010009386304.

Schultz, M.P., Walker, J.M., Steppe, C.N., Flack, K.A., 2015. Impact of diatomaceous biofilms on the frictional drag of fouling-release coatings. Biofouling 31 (9–10), 759–773. https://doi.org/10.1080/08927014.2015.1108407.

Song, S., Dai, S., Demirel, Y.K., Atlar, M., Day, S., Turan, O., 2021a. Experimental and theoretical study of the effect of hull roughness on ship resistance. J. Ship Res. 65 (1), 62–71. https://doi.org/10.5957/JOSR.07190040.

Song, S., Demirel, Y.K., Atlar, M., 2019. An investigation into the effect of biofouling on the ship hydrodynamic characteristics using CFD. Ocean Eng. 175, 122–137. https://doi.org/10.1016/j.oceaneng.2019.01.056.

Song, S., Demirel, Y.K., Atlar, M., 2020a. Penalty of hull and propeller fouling on ship self-propulsion performance. Appl. Ocean Res. 94, 102006 https://doi.org/10.1016/j.apor.2019.102006.

Song, S., Demirel, Y.K., Atlar, M., 2020b. Propeller performance penalty of biofouling: computational fluid Dynamics prediction. J. Offshore Mech. Arctic Eng. 142 (6) https://doi.org/10.1115/1.4047201.

Song, S., Demirel, Y.K., Atlar, M., Dai, S., Day, S., Turan, O., 2020c. Validation of the CFD approach for modelling roughness effect on ship resistance. Ocean Eng. 200, 107029 https://doi.org/10.1016/j.oceaneng.2020.107029.

Song, S., Demirel, Y.K., Atlar, M., Shi, W., 2020d. Prediction of the fouling penalty on the tidal turbine performance and development of its mitigation measures. Appl. Energy 276, 115498. https://doi.org/10.1016/j.apenergy.2020.115498.

Song, S., Demirel, Y.K., De Marco Muscat-Fenech, C., Tezdogan, T., Atlar, M., 2020e. Fouling effect on the resistance of different ship types. Ocean Eng. 216, 107736 https://doi.org/10.1016/j.oceaneng.2020.107736.

Song, S., Demirel, Y.K., Muscat-Fenech, C.D.M., Sant, T., Villa, D., Tezdogan, T., Incecik, A., 2021b. Investigating the effect of heterogeneous hull roughness on ship resistance using CFD. J. Mar. Sci. Eng. 9 (2), 202. https://www.mdpi.com/2077-1312/9/2/202.

Song, S., Ravenna, R., Dai, S., DeMarco Muscat-Fenech, C., Tani, G., Demirel, Y.K., Atlar, M., Day, S., Incecik, A., 2021c. Experimental investigation on the effect of heterogeneous hull roughness on ship resistance. Ocean Eng. 223, 108590 https://doi.org/10.1016/j.oceaneng.2021.108590.

Suastika, I.K., Hakim, M.L., Nugroho, B., Nasirudin, A., Utama, I.K.A.P., Monty, J.P., Ganapathisubramani, B., 2021. Characteristics of drag due to streamwise inhomogeneous roughness. Ocean Eng. 223, 108632 https://doi.org/10.1016/j.oceaneng.2021.108632.

Turan, O., Demirel, Y.K., Day, S., Tezdogan, T., 2016. Experimental determination of added hydrodynamic resistance caused by marine biofouling on ships. Transport. Res. Procedia 14, 1649–1658. https://doi.org/10.1016/j.trpro.2016.05.130.

Uzun, D., Demirel, Y.K., Coraddu, A., Turan, O., 2019a. *Life Cycle Assessment of an Antifouling Coating Based on Time-dependent Biofouling Model* 18th Conference on Computer Applications and Information Technology in the Maritime Industries. Tullamore, Ireland.

Uzun, D., Demirel, Y.K., Coraddu, A., Turan, O., 2019b. Time-dependent biofouling growth model for predicting the effects of biofouling on ship resistance and powering. Ocean Eng. 191, 106432 https://doi.org/10.1016/j.oceaneng.2019.106432.

Uzun, D., Ozyurt, R., Demirel, Y.K., Turan, O., 2020. Does the barnacle settlement pattern affect ship resistance and powering? Appl. Ocean Res. 95, 102020 https://doi.org/10.1016/j.apor.2019.102020.

Van, S.-H., Ahn, H., Lee, Y.-Y., Kim, C., Hwang, S., Kim, J., Kim, K.-S., Park, I.-R., 2011. Resistance Characteristics and Form Factor Evaluation for Geosim Models of KVLCC2 and KCS, 4-6 April). The 2nd International Conference on Advanced Model Measurement Technology for the EU Maritime Industry, Newcastle upon Tyne, UK.